Entorhinal Grid Cells May Facilitate Pattern Separation in the Hippocampus

Jochen Kerdels and Gabriele Peters
University of Hagen, Universitätsstrasse 1, D-58097 Hagen, Germany

Keywords: Pattern Separation, Grid Cells, Entorhinal Cortex, Dentate Gyrus, Hippocampus.

Abstract: The dentate gyrus (DG) in the hippocampus of the mammalian brain is known to exhibit strong pattern separation. However, how this pattern separation arises in the DG is not well understood. Here we offer a novel hypothesis regarding this problem by demonstrating that pattern separation can already be performed by entorhinal grid cells, which are located just one synapse upstream of the DG. For our simulations we utilize a recently introduced grid cell model that interprets the behavior of grid cells as just one instance of a general information processing scheme. The obtained results challenge the established view that pattern separation occurs primarily in the DG, and they uncover a common misconception regarding the specificity of ensemble activity in grid cells.

1 INTRODUCTION

The parahippocampal region (PHR) and the hippocampal formation (HF) in the mammalian brain are vital for storing and retrieving episodic memories, i.e., memories of specific events experienced by the organism (Tulving and Markowitsch, 1998; Burgess et al., 2002; Rolls, 2013). A key requirement for this kind of memory is the ability to distinguish between similar events that may differ only in minute details. To accomplish such differentiation it is commonly assumed that parts of the hippocampus carry out some form of pattern separation that orthogonalizes the input signals before they are stored in an autoassociative memory (Leutgeb et al., 2007; Yassa and Stark, 2011; Rolls, 2013). As a result of this pattern separation, similar input signals cause divergent sets of neurons to become active and thus reduce confusion of these inputs in subsequent processing steps. Within the hippocampus such divergent activation of neurons in response to similar inputs was primarily observed in the dentate gyrus (DG) (Leutgeb et al., 2007; Berron et al., 2016). However, how this observed pattern separation in the DG arises is not well understood (Rolls, 2013).

In this paper we offer a novel hypothesis regarding this problem. Based on our recently introduced computational model of entorhinal grid cells (Kerdels and Peters, 2015; Kerdels, 2016) we will show that the behavior of grid cells – if it is interpreted as an instance of a general information processing scheme – already results in strong pattern separation within the entorhinal cortex (EC). As the latter provides the main input to the dentate gyrus (van Strien et al., 2009) we hypothesize that the pattern separation observed in DG is facilitated by output signals from the EC that are already well separated and that the DG itself just improves this separation by sparsification.

The next two sections provide a brief overview of the parahippocampal-hippocampal network (PHR-HF) and our computational model of entorhinal grid cells. Section 4 outlines the experimental setup and characterizes the input signal used in the simulations. In sections 5 and 6 we present and discuss the simulation results.

2 PHR-HF OVERVIEW

The parahippocampal-hippocampal region of the mammalian brain is part of the limbic system. It has a long evolutionary history and putative homologues can be found in most vertebrate species (Butler and Hodos, 2005). Functionally, the region is necessary for short term and declarative memory, which includes factual knowledge as well as episodic memories (Squire et al., 2008).

The parahippocampal region (PHR) consists of five main areas designated as perirhinal cortex (PER), postrhinal cortex (POR), presubiculum (PrS), para-

Kerdels J. and Peters G.
Entorhinal Grid Cells May Facilitate Pattern Separation in the Hippocampus.
DOI: 10.5220/0006514601410148
In *Proceedings of the 9th International Joint Conference on Computational Intelligence (IJCCI 2017)*, pages 141-148
ISBN: 978-989-758-274-5

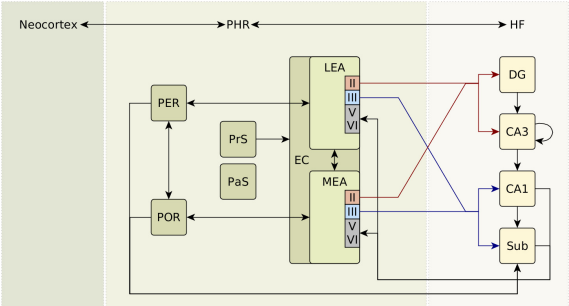

Figure 1: The standard view of the parahippocampal-hippocampal network based on the review by (van Strien et al., 2009).

subiculum (PaS), and entorhinal cortex (EC). The latter being further subdivided into a lateral (LEA) and a medial (MEA) part. The areas of the PHR have six layers similar to the neocortex with layers II/III and layers V/VI being the principal cell layers that contain the majority of neuronal cell bodies. The hippocampal formation (HF) consists of four main areas designated as dentate gyrus (DG), cornu ammonis 3 (CA3), cornu ammonis 1 (CA1), and subiculum (Sub). In contrast to the PHR and the neocortex the areas of the HF have only three layers, with the central layer containing the majority of cell bodies (Witter et al., 2000; Squire et al., 2008; van Strien et al., 2009; Somogyi, 2010).

Figure 1 outlines the basic PHR-HF network. It shows that the PHR acts as a gateway that mediates both the input from the neocortex to the HF, as well as the output from the HF to the neocortex. Two major, bidirectional projection streams facilitate this exchange of signals. The PER connects predominantly with the LEA, while the POR connects to the MEA. From the upper layers II/III of the EC the so called *perforant pathway* projects then to all areas of the HF. Signals from the second layer reach the DG and CA1, whereas signals from the third layer go to CA1 and the subiculum. The output from the HF projects from areas CA1 and the subiculum to deep layers V/VI of the EC (van Strien et al., 2009). As a rough approximation the hippocampus can be interpreted as a sequence of processing modules, starting with the DG and ending with the subiculum, that receives inputs from the upper layers of the EC and feeds its results back to the lower layers of the EC. As such, the EC can be interpreted as the main interface to the hippocampus.

A major advance in the understanding of EC function resulted from the discovery of *grid cells* and their subsequent investigation (Fyhn et al., 2004; Hafting et al., 2005; Rowland et al., 2016). The activity of grid cells correlates strongly with the animal's location creating a hexagonal pattern of firing fields that spans the entire environment of the animal. This strong spatial correlation provides a rare opportunity to experimentally observe and interpret the behavior of neurons in this part of the brain. Common hypothesis regarding the function of grid cells view these cells as specialized components in a system facilitating orientation and navigation (Rowland et al., 2016). However, recent observations of grid like firing patterns in contexts other than locomotion (Killian et al., 2012; Constantinescu et al., 2016; Aronov et al., 2017; Diehl et al., 2017) may indicate that the behavior of grid cells reflects a more general, underlying processing scheme. To investigate this hypothesis we developed a computational model of grid cells that implements such a general processing scheme allowing us to apply our model outside of the typical context of navigation and orientation (Kerdels and Peters, 2015; Kerdels, 2016; Kerdels and Peters, 2016). We briefly outline the model in the next section.

3 GRID CELL MODEL

We developed our grid cell model based on the idea that the behavior observed in grid cells is just one instance of a more general information processing scheme. We hypothesize that grid cells form a simple, piecewise representation of their *entire* input space by learning a limited number of input patterns or *prototypes* that reflect the input space structure. Simultaneously, competition among cells within a local grid cell group ensures that the simple representations learned by the individual cells are pairwise distinct and interleave in such a way that a complex representation of the input space emerges that is distributed over the entire group of neurons.

On the neurobiological level such a prototype-based representation could be stored within the dendritic tree of a neuron with individual prototypes being stored in local dendritic subsections. In our model we utilize the core ideas of the growing neural gas (GNG) algorithm to describe this learning process. The GNG is an unsupervised learning algorithm that uses biologically plausible competitive Hebbian learning to approximate the input space structure with a network of prototypes (Martinetz and Schulten, 1994; Fritzke, 1995). We extended the regular GNG algorithm into a recursive version (RGNG) that allows us to simultaneously describe both the learning processes of individual neurons as well as the competition among a group of neurons by the same GNG dynamics. For a formal description and an in-depth characterization of the model we refer to (Kerdels and Peters, 2016; Kerdels, 2016).

Figure 2: Typical samples of the digit 8 in the MNIST database of handwritten digits (Lecun et al., 1998).

Regarding this work, the most important property of the RGNG-based grid cell model is its ability to operate on *arbitrary* input spaces. Regardless of the particular input space, e.g., the modality or dimension of the input signals, the modeled group of neurons will try to learn the structure of that input space as well as possible. In addition, as each neuron tries to learn the structure of the *entire* input space the learned representations of different neurons will be self-similar and no individual neuron will "specialize" on a particular region of input space. As a consequence, small shifts of the input signal are likely to cause a significant change in the set of active cells in the modeled neuron group, hence effectively implementing a form of pattern separation.

4 EXPERIMENTAL SETUP

To investigate the potential pattern separation capabilities of grid cells we simulated multiple groups of grid cells using the RGNG-based grid cell model and exposed these groups to a sequence of input samples from a given input space. For each input sample the resulting activity of each simulated grid cell was determined and the individual activities within a grid cell group were then summarized in an *activity vector*. This vector can be interpreted as the grid cell group's encoding of the respective input sample. To compare this encoding with the original encoding of the input signal in terms of orthogonality we decided to use the cosine similarity measure, as it is a direct measure of the (non-)orthogonality of two vectors.

As input space we chose the well-known MNIST database of handwritten digits (Lecun et al., 1998), which provides a total of 60000 samples of handwritten digits in the resolution of $28 \times 28 = 784$ pixels. Since the intra-class samples in this database exhibit a high degree of similarity (Fig. 2) it is especially suited to investigate the pattern separation capabilities of an encoding scheme. Figure 3 shows the intra- and inter-class cosine similarity distributions in the MNIST dataset. Cosine similarity values close to 0 indicate orthogonal vectors, while values close to 1 indicate a high degree of similarity. For any encoding that performs pattern separation it is expected that corresponding distributions of the encoded signals will be skewed towards 0.

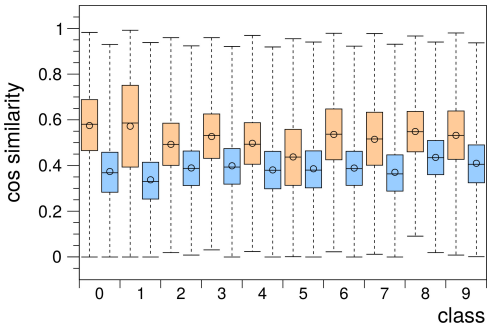

Figure 3: Box plot of the intra-class (orange, left columns) and inter-class (blue, right columns) cosine similarity distributions occurring in the MNIST dataset. Bottom and top of dashed lines represent minimum and maximum values, bottom and top of each box represent lower and upper quartiles, thick lines represent medians, and circles represent mean values of the distributions.

A total of 15 grid cell groups were simulated. Each group consisted of 100 neurons and received 2.88 million (partial) input samples from the MNIST input space, i.e., 48 repetitions of 60000 samples. Thus, the activity vectors derived from each group were 100-dimensional. The grid cell groups differed by the number $\{20, 40, 80\}$ of prototypes each neuron was allowed to use for its input space representation, and by processing either entire input samples or just the top, bottom, left, or right half of the samples. The number of prototypes per cell influences the "resolution" with which the cell can form an input space representation. A lower number of prototypes results in a more coarse representation, i.e., grid cells with a low number of prototypes have larger *grid spacing* than grid cells with a high number of prototypes. The numbers of prototypes used here were chosen from a range that is biologically plausible (Kerdels, 2016). The processing of partial input samples was used as a proxy for simulating multimodal input, i.e., as input that usually occurs together but that is represented and encoded by independent groups of neurons. All other parameters of the RGNG-based grid cell model were held constant and are provided in the appendix.

5 RESULTS

Figure 4 shows the intra- and inter-class cosine similarity distributions occurring in the activity vectors of grid cell groups that processed 2.88 million input samples from the MNIST input space and used either 20, 40, or 80 prototypes per cell for their input space representation. The activity vectors were

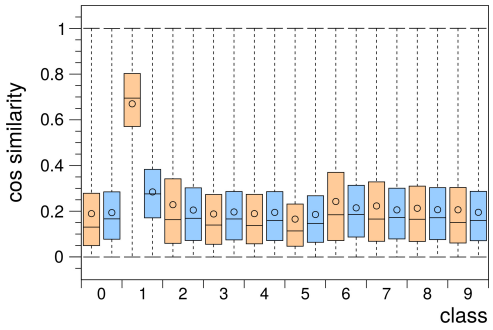

(a) 20 prototypes per cell

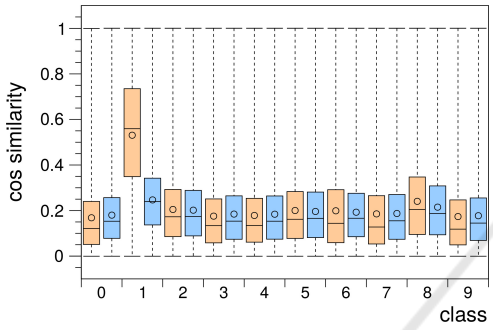

(b) 40 prototypes per cell

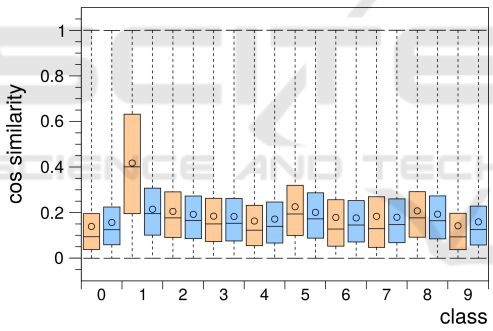

(c) 80 prototypes per cell

Figure 4: Box plots as in figure 3 of the intra- and inter-class cosine similarity distributions occurring in the activity vectors of grid cell groups using 20 (**a**), 40 (**b**), or 80 (**c**) prototypes per cell for their input space representation.

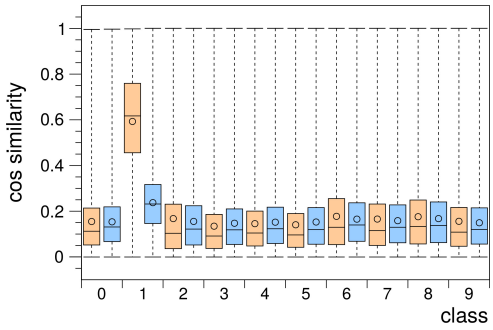

(a) combined groups 20 and 40 prot.

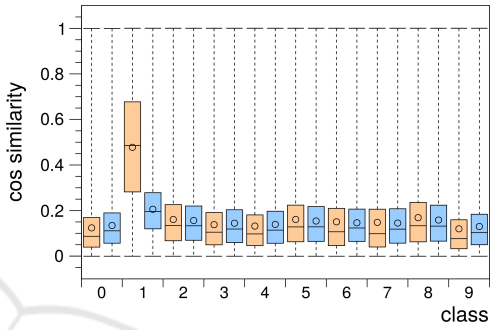

(b) combined groups 40 and 80 prot.

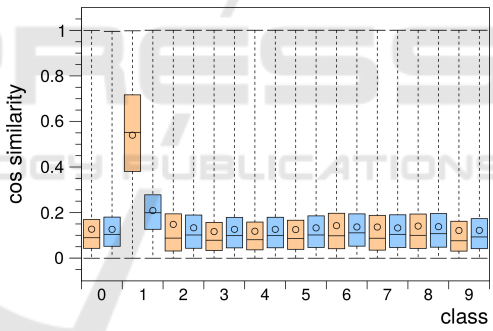

(c) combined groups 20, 40, and 80 prot.

Figure 5: Box plots as in figure 3 of the intra- and inter-class cosine similarity distributions occurring in **combined** activity vectors of grid cell groups. (**a**) Two grid cell groups using 20 and 40 prototypes per cell. (**b**) Two grid cell groups using 40 and 80 prototypes per cell. (**c**) Three grid cell groups using 20, 40, and 80 prototypes per cell.

sampled during the 48th input repetition of the 60000 MNIST training samples. For most classes the distributions show a significant decrease in the cosine similarities when compared with the cosine similarities measured in the MNIST set (Fig. 3). Mean values for both intra- and inter-class similarities dropped from about 0.5 and 0.4, respectively, to about 0.2. In addition, the clear difference of similarity values between intra- and inter-class distributions visible in the MNIST set was equalized in the grid cell group activity vectors. Notably, the intra-class distribution of class 1 deviates from these observations. It is broader and retains a relatively high median similarity value. In the case of the grid cell group that only uses 20 prototypes per cell the median value has even increased rather than decreased when compared to the MNIST set median value of class 1. These deviations of the class 1 distributions can be attributed to the fact that the digit one is typically drawn as just a vertical stroke with little variation.

It is a common notion within the grid cell literature that the output signals of entorhinal grid cell groups that exhibit different grid spacings combine in the hippocampus to uniquely encode specific places in an animal's environment (Solstad et al., 2006). To investigate the orthogonality of such combined output signals we concatenated the activity vectors of two or more simulated grid cell groups that use different numbers of prototypes per cell and analysed the resulting intra- and inter-class cosine similarity distributions. Figure 5 shows the distributions occurring in the combined activity vectors of groups using 20 and 40 prototypes (Fig. 5a), 40 and 80 prototypes (Fig. 5b), as well as 20, 40, and 80 prototypes (Fig. 5c). In general, the results are qualitatively similar to that from the non-combined, individual grid cell groups (Fig. 4), though the widths of the distributions as well as the mean similarity values have slightly decreased.

A different source of combined output signals can be multimodal input. The entorhinal cortex receives projections from various areas of the neocortex and the limbic system. This multimodal input is then processed and forwarded to the hippocampus. To simulate input from multiple modalities we split the MNIST input samples into top, bottom, left, and right halves and let these partial samples be processed by four separate grid cell groups. The activity vectors of these four groups were then concatenated and analysed. Figure 6 shows the intra- and inter-class cosine similarity distributions occurring in combined activity vectors of groups that used 20 (Fig. 6a), 40 (Fig. 6b), and 80 (Fig. 6c) prototypes per cell. In all three cases there is a much more pronounced reduction in the widths of the distributions and the mean similarity values as compared to the distributions occurring in the combined activity vectors of grid cell groups with different grid spacings (Fig. 5). The lowest mean similarity values of about 0.05 are achieved by the four grid cell groups that use 80 prototypes per cell for their input space representation. Remarkably, even the mean similarity value of the intra-class distribution of class 1 decreases in this multimodal setting down to a value of about 0.25 from about 0.6 measured in the MNIST set.

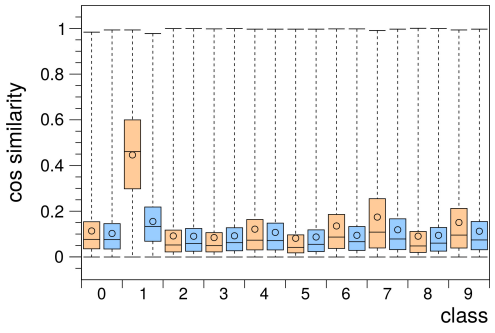

(a) multi modal / 20 prototypes

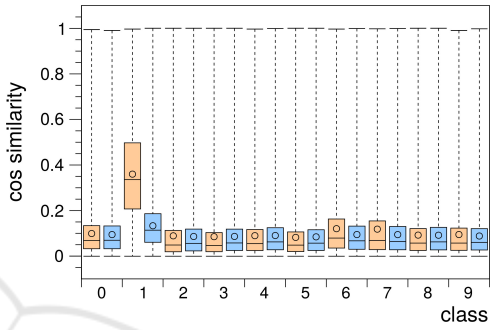

(b) multi modal / 40 prototypes

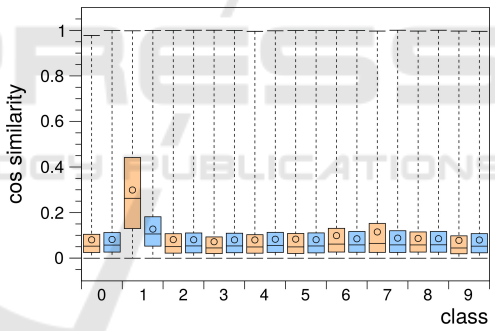

(c) multi modal / 80 prototypes

Figure 6: Box plots as in figure 3 of the intra- and inter-class cosine similarity distributions occurring in simulated **multimodal** activity vectors of grid cell groups encoding the top, bottom, left, or right halves of the MNIST input samples using 20 (**a**), 40 (**b**), or 80 (**c**) prototypes per cell.

6 DISCUSSION

The results presented in the previous section indicate that – under the given hypothesis – entorhinal grid cells perform pattern separation on their input signals and provide already orthogonalized output signals to the hippocampus. This result provides a novel perspective on the possible genesis of the pattern separation that can be observed in the dentate gyrus (Leutgeb et al., 2007; Berron et al., 2016). From this perspective, the input signals to the DG may already be well separated and the pattern separation observed in the DG may just be a result of further sparsification, e.g., due to the neurogenesis occurring in this region. Furthermore, shifting the "functionality" of pattern separation from DG to EC would provide orthogonalized inputs not only to the DG but also to all other parts of the hippocampus (Fig. 1). This shift would

improve the support of hippocampal memory models that assume that memory retrieval can operate without the involvement of the DG (Tulving and Markowitsch, 1998).

Another important aspect is the observation that pattern separation does not require the collaboration of multiple grid cell groups (Fig. 4). A typical grid cell fires if the animal is at one of multiple locations. In terms of the RGNG-based grid cell model the grid cell fires if the input to the cell matches one of its multiple prototypes. Thus, from the activity of a single grid cell it is not possible to derive which of the prototypes caused the cell to fire. The input pattern could be similar to any of the multiple patterns encoded in the prototypes (Fig. 7). Within a grid cell group the prototypes of grid cells are typically shifted against each other. In most grid cell models found in the literature this property is described in an idealized way such that the relative locations of firing fields, i.e., the prototypes of all grid cells in the group are precisely aligned. In this idealized case the joint activity of the grid cell group remains ambiguous with respect to the actual input pattern. However, in reality the alignment of firing patterns in a grid cell group is less precise and can exhibit local permutations of the cell's firing fields. As a consequence, these permutations make the joint activity of a grid cell group much more specific and less ambiguous than is commonly thought. The RGNG-based grid cell model allows for such natural variation in the alignment, and the resulting specificity of the grid cell group activity is reflected by the high degree of pattern separation present in the inter-class distributions shown in figure 4.

A third important result is the observation that the joint activity of grid cell groups that process different modalities (Fig. 6) shows a much stronger pattern separation than the joint activity of grid cell groups that have different grid spacings (Fig. 5). Yet, the grid cell literature focuses much more on the latter (Rolls et al., 2006; Solstad et al., 2006; Franzius et al., 2007; de Almeida et al., 2009; Savelli and Knierim, 2010), while aspects of multimodality appear to be underrepresented (Aronov et al., 2017; Diehl et al., 2017).

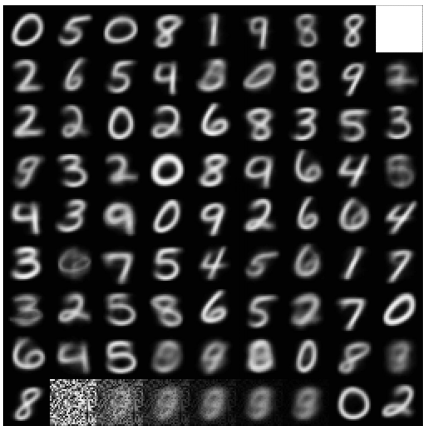

(a) cell #1

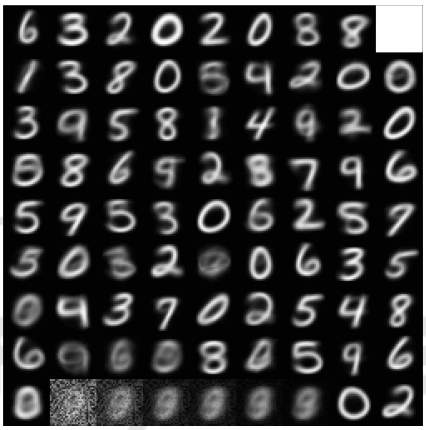

(b) cell #10

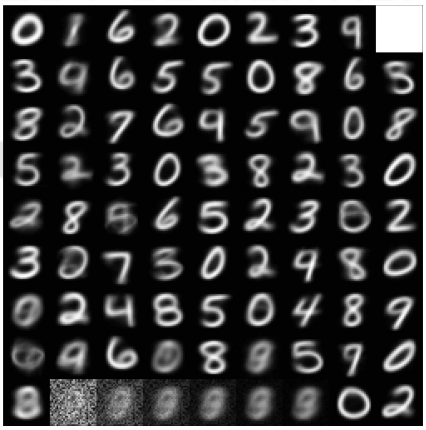

(c) cell #20

Figure 7: Three examples of 80 prototypes that were learned by three grid cells {#1,#10,#20} to form an input space representation. The prototypes typically cover the entire input space in each grid cell and are slightly shifted in the input space across different cells. The last rows in the prototype overviews show examples of "unused" prototypes that the cells haven't utilized so far.

7 CONCLUSION

We investigated the degree to which entorhinal grid cells perform pattern separation and thus may facilitate the subsequent pattern separation observed in areas of the hippocampus. Based on the hypothesis that the behavior of entorhinal grid cells is just one instance of a more general information process-

ing scheme we used our recently introduced RGNG-based grid cell model (Kerdels and Peters, 2015; Kerdels, 2016; Kerdels and Peters, 2016) to simulate several groups of grid cells that processed visual inputs derived from the MNIST database of handwritten digits. The results indicate that entorhinal grid cells may indeed perform pattern separation on their input signals and thus may provide already orthogonalized output signals to the hippocampus.

These results challenge established views on the parahippocampal-hippocampal region and provide a novel explanation for the origin of the pattern separation that is observed in the dentate gyrus. Furthermore, they uncover a common misconception about the assumed lack of specificity in the activity of grid cell groups. Finally, the results encourage the further investigation of the influence of multimodal input on the processing within the entorhinal cortex.

REFERENCES

Aronov, D., Nevers, R., and Tank, D. W. (2017). Mapping of a non-spatial dimension by the hippocampal–entorhinal circuit. *Nature*, 543(7647):719–722.

Berron, D., Schütze, H., Maass, A., Cardenas-Blanco, A., Kuijf, H. J., Kumaran, D., and Düzel, E. (2016). Strong evidence for pattern separation in human dentate gyrus. *Journal of Neuroscience*, 36(29):7569–7579.

Burgess, N., Maguire, E. A., and O'Keefe, J. (2002). The human hippocampus and spatial and episodic memory. *Neuron*, 35(4):625 – 641.

Butler, A. and Hodos, W. (2005). *Comparative Vertebrate Neuroanatomy: Evolution and Adaptation*. Wiley.

Constantinescu, A. O., O'Reilly, J. X., and Behrens, T. E. J. (2016). Organizing conceptual knowledge in humans with a grid-like code. *Science (New York, N.Y.)*, 352(6292):1464–1468.

de Almeida, L., Idiart, M., and Lisman, J. E. (2009). The inputoutput transformation of the hippocampal granule cells: From grid cells to place fields. *The Journal of Neuroscience*, 29(23):7504–7512.

Diehl, G. W., Hon, O. J., Leutgeb, S., and Leutgeb, J. K. (2017). Grid and nongrid cells in medial entorhinal cortex represent spatial location and environmental features with complementary coding schemes. *Neuron*, 94(1):83 – 92.e6.

Franzius, M., Vollgraf, R., and Wiskott, L. (2007). From grids to places. *Journal of Computational Neuroscience*, 22(3):297–299.

Fritzke, B. (1995). A growing neural gas network learns topologies. In *Advances in Neural Information Processing Systems 7*, pages 625–632. MIT Press.

Fyhn, M., Molden, S., Witter, M. P., Moser, E. I., and Moser, M.-B. (2004). Spatial representation in the entorhinal cortex. *Science*, 305(5688):1258–1264.

Hafting, T., Fyhn, M., Molden, S., Moser, M.-B., and Moser, E. I. (2005). Microstructure of a spatial map in the entorhinal cortex. *Nature*, 436(7052):801–806.

Kerdels, J. (2016). *A Computational Model of Grid Cells based on a Recursive Growing Neural Gas*. PhD thesis, FernUniversität in Hagen, Hagen.

Kerdels, J. and Peters, G. (2015). A new view on grid cells beyond the cognitive map hypothesis. In *8th Conference on Artificial General Intelligence (AGI 2015)*.

Kerdels, J. and Peters, G. (2016). Modelling the grid-like encoding of visual space in primates. In *Proceedings of the 8th International Joint Conference on Computational Intelligence, IJCCI 2016, Volume 3: NCTA, Porto, Portugal, November 9-11, 2016.*, pages 42–49.

Killian, N. J., Jutras, M. J., and Buffalo, E. A. (2012). A map of visual space in the primate entorhinal cortex. *Nature*, 491(7426):761–764.

Lecun, Y., Bottou, L., Bengio, Y., and Haffner, P. (1998). Gradient-based learning applied to document recognition. *Proceedings of the IEEE*, 86(11):2278–2324.

Leutgeb, J. K., Leutgeb, S., Moser, M.-B., and Moser, E. I. (2007). Pattern separation in the dentate gyrus and ca3 of the hippocampus. *Science*, 315(5814):961–966.

Martinetz, T. M. and Schulten, K. (1994). Topology representing networks. *Neural Networks*, 7:507–522.

Rolls, E. (2013). The mechanisms for pattern completion and pattern separation in the hippocampus. *Frontiers in Systems Neuroscience*, 7(74).

Rolls, E. T., Stringer, S. M., and Elliot, T. (2006). Entorhinal cortex grid cells can map to hippocampal place cells by competitive learning. *Network: Computation in Neural Systems*, 17(4):447–465. PMID: 17162463.

Rowland, D. C., Roudi, Y., Moser, M.-B., and Moser, E. I. (2016). Ten years of grid cells. *Annual Review of Neuroscience*, 39(1):19–40. PMID: 27023731.

Savelli, F. and Knierim, J. J. (2010). Hebbian analysis of the transformation of medial entorhinal grid-cell inputs to hippocampal place fields. *Journal of Neurophysiology*, 103(6):3167–3183.

Solstad, T., Moser, E. I., and Einevoll, G. T. (2006). From grid cells to place cells: A mathematical model. *Hippocampus*, 16(12):1026–1031.

Somogyi, P. (2010). Hippocampus: Intrinsic organization. In Shepherd, G. M. and Grillner, S., editors, *Handbook of Brain Microcircuits*, pages 148–164. Oxford University Press.

Squire, L., Bloom, F., Spitzer, N., Squire, L., Berg, D., du Lac, S., and Ghosh, A. (2008). *Fundamental Neuroscience*. Fundamental Neuroscience Series. Elsevier Science.

Tulving, E. and Markowitsch, H. J. (1998). Episodic and declarative memory: Role of the hippocampus. *Hippocampus*, 8(3):198–204.

van Strien, N. M., Cappaert, N. L. M., and Witter, M. P. (2009). The anatomy of memory: an interactive overview of the parahippocampal-hippocampal network. *Nat Rev Neurosci*, 10(4):272–282.

Witter, M. P., Wouterlood, F. G., Naber, P. A., and van Haeften, T. (2000). Anatomical organization of the

parahippocampal-hippocampal network. *Annals of the New York Academy of Sciences*, 911(1):1–24.

Yassa, M. A. and Stark, C. E. L. (2011). Pattern separation in the hippocampus. *Trends in neurosciences*, 34(10):515–525.

APPENDIX

Parameterization

Each layer of an RGNG requires its own set of parameters. In case of our two-layered grid cell model we use the sets of parameters θ_1 and θ_2, respectively. Parameter set θ_1 controls the main top layer RGNG while parameter set θ_2 controls all bottom layer RGNGs. Table 1 summarizes the parameter values used for the simulation runs presented in this paper. For a detailed characterization of these parameters we refer to Kerdels (Kerdels, 2016).

Table 1: Parameters of the RGNG-based model used throughout all simulation runs. Parameters θ_1 control the top layer RGNG while parameters θ_2 control all bottom layer RGNGs of the model.

θ_1			θ_2		
ε_b	=	0.004	ε_b	=	0.001
ε_n	=	0.004	ε_n	=	0.00001
ε_r	=	0.01	ε_r	=	0.01
λ	=	1000	λ	=	1000
τ	=	300	τ	=	300
α	=	0.5	α	=	0.5
β	=	0.0005	β	=	0.0005
M	=	100	M	=	$\{20, 40, 80\}$